JOURNAL OF AIRCRAFT
Vol. 35, No. 5, September–October 1998

Numerical Simulation of Flowfield Around Airfoil with Stationary or Oscillating Spoiler

Ji Hong Kim* and Oh Hyun Rho†
Seoul National University, Seoul 151-742, Republic of Korea

Flow around an airfoil with a stationary or oscillating spoiler has been numerically simulated by solving the unsteady turbulent compressible two-dimensional, full Navier–Stokes equations. In the stationary spoiler case computations were carried out at three spoiler deflection angles, 15, 30, and 60 deg. The results were compared with the existing experimental data and showed good agreement. To analyze the complex unsteady flow induced by the relative motion of two rigidly connected bodies, an overlapped-dynamic, grid-generation method has been developed and applied to the oscillating spoiler problem. The effects of the reduced frequency and the amplitude of the oscillating spoiler were investigated and the potential capability of the oscillating spoiler for the application of active control technology was demonstrated.

Nomenclature

C_s = spoiler chord
h = spoiler projection height on airfoil trailing edge
K = reduced frequency based on spoiler chord, $2\pi f C_s/U_\infty$
l_j^n = normal distance from $\boldsymbol{X}_j$ to $\boldsymbol{X}_{bf}$
l_j^t = projection length of $\boldsymbol{X}_{bj}$ on $\boldsymbol{X}_{bf}$
St_h = Strouhal number based on spoiler projection height, fh/U_∞
$\hat{\boldsymbol{u}}_n$ = unit normal vector of $\boldsymbol{X}_{bf}$
$\hat{\boldsymbol{u}}_t$ = unit tangential vector of $\boldsymbol{X}_{bf}$
δ_i = amplitude of oscillation
δ_m = mean deflection angle of oscillating spoiler
δ_s = deflection angle of steady spoiler

Subscripts
b, f = boundary grid point of arbitrary grid line
$0, f, 1$ = Strouhal, forced, and dominant frequency

Introduction

SPOILERS are well-known aerodynamic control devices that are mainly used as aerodynamic brakes or lift dumpers at touchdown. They can also be used as effective control devices during flight when combined with the movement of ailerons. Recent progress in active control technology (ACT) suggests that spoilers have the potential to control unsteady aerodynamic loads such as flutter and buffet suppression or gust load alleviation.[1]

Previous researches on the unsteady flows generated by a spoiler are usually categorized into three groups. The first group is mainly focused on the stationary spoiler. Most of the researches were conducted experimentally with the model of the Boeing advanced transport research (BATR) airfoil.[2–7] In a series of experiments the flowfield including the wake region was measured, and the turbulence characteristics and the effects of the geometrical design variables were studied. The results provided a good experimental database to be compared with the computational results. However, the quantitative data should be treated cautiously because of the scale and wind-tunnel blockage effects. Most theoretical studies adopted the discrete vortex method. Ok and Eberhardt[8] performed incompressible Navier–Stokes calculations.

The second group is focused on the oscillating spoiler. Costes et al.[9] and Consigny et al.[10] performed experiments in transonic speed to understand the performance of an oscillating spoiler. However, their experiments are confined to the small spoiler deflection angle and the relatively low reduced frequency range. Furthermore, the basic airfoil shape is not known, and so a direct comparison with the computation is not possible. There was also research on the oscillating spoiler-like control devices, for the purpose of reducing the separated flow region.[11]

The third group is mainly interested in the rapidly deployed spoiler. The unsteady phenomenon related to this topic is the formation of the strong dynamic stall vortex that results in short-term lift augmentation. This phenomenon has a mechanism similar to the dynamic stall vortex of the pitching or ramp motion of an airfoil. This aspect of the spoiler is undesirable as a speed brake or a lift dumper, and it is named *adverse lift*. Jordan et al.[12] attempted to eliminate this phenomenon. However, Consigny et al.[10] and Mabey[13,14] recognized that these large unsteady aerodynamic loads could be used for the ACT of a highly maneuverable aircraft if they could be controlled. Only a limited amount of research exists on this subject. Some numerical applications using the discrete vortex method are not adequate for a thorough understanding of the flowfield. The problem still remains as one of the challenging subjects in computational fluid dynamics (CFD) in the aspect of a grid method, an appropriate turbulence model in a massively separated unsteady flow, and an efficient time-integration method.

Recent progress in CFD has made it possible to calculate the flowfield around complex geometry and unsteady flow induced by the relative motion between bodies. One popular grid method to solve the flowfield around complex bodies is an overlapping grid scheme known as chimera. A chimera grid scheme is particularly suited for solving moving body problems such as launch-vehicle staging, aircraft-store separation, and helicopter-rotor/body interaction.[15,16] One simple assump-

Presented as Paper 96-2509 at the AIAA 14th Applied Aerodynamics Conference, New Orleans, LA, June 17–20, 1996; received Nov. 26, 1996; revision received Feb. 25, 1998; accepted for publication March 4, 1998.

*Graduate Research Assistant, Department of Aerospace Engineering; currently Senior Research Engineer, Aerospace R&D Center, Daewoo Heavy Industries Ltd., Changwon 641-120, Republic of Korea.

†Professor, Department of Aerospace Engineering. Senior Member AIAA.

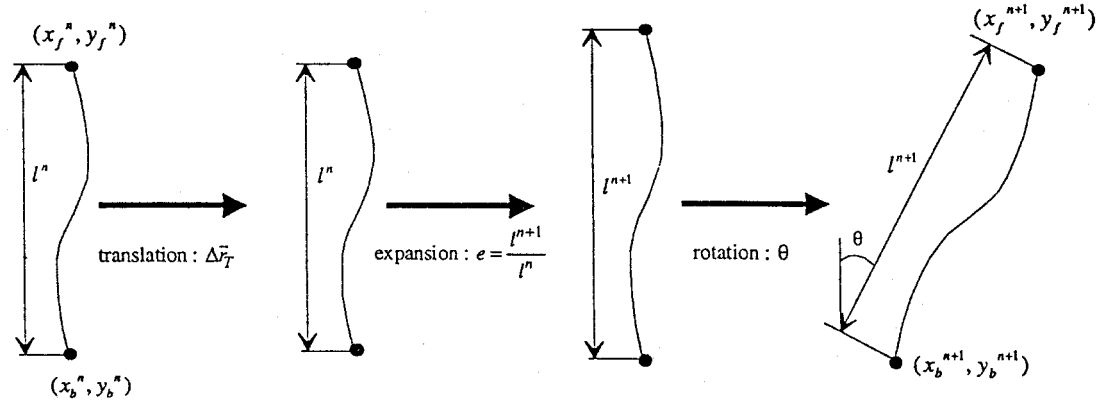

Fig. 1 Procedure of flexible dynamic grid generation.

tion behind this technique is that each grid system moves rigidly without any deformation of the body or inner grid. However, when relative motion exists between two connected bodies, such as an oscillating spoiler with an airfoil, independent grid motion is impossible. Because there is a region in which the hole of each grid overlaps because of the body connection, data communication is impossible; hence, a dynamically deformed grid is inevitable. The previous researches on a dynamic grid method usually utilized regridding at each time step and determined grid speed by a backward-difference method. It requires much computation time and lacks accuracy because of errors involved in the backward-difference method. One interesting and efficient dynamic grid generation method proposed by Kim and Lee[17] showed the possibility of solving the problem of relative motion between two bodies with grid deformation. However, Kim and Lee employed this method with a blocked grid, which has limitations for the large displacement motion. Therefore, it is natural to develop the grid method that retains the merits of both schemes. In this paper the flexible motion of subgrid enabled the removal of any constraints of a chimera or a blocked grid scheme. The motion of the grid is analogous to that of the folding–unfolding fan, so this dynamic overlapped grid method can solve the problem of large displacement spoiler oscillation. Also, it has the ability to solve the rapid deploying and contracting spoiler from the initial part of an airfoil surface. A specific objective of this study is to provide a better understanding of the physics of the unsteady flowfield induced by the stationary or oscillating spoiler. Numerical investigations are carried out by solving unsteady, two-dimensional, turbulent Navier–Stokes equations. Attention is paid to the variation of a steady spoiler deflection angle and the effects of reduced frequency and amplitude of spoiler oscillation.

Numerical Method

The governing equations are two-dimensional, unsteady, full Navier–Stokes equations and are expressed as the following strong conservative form in generalized coordinates:

$$\partial_t \hat{Q} + \partial_\xi(\hat{E} - \hat{E}_v) + \partial_\eta(\hat{F} - \hat{F}_v) = 0 \tag{1}$$

For the time-accurate calculation the alternating direction implicit (ADI) scheme with Newton subiteration is used. With a second-order time accuracy and nonconstant time step the equations can be represented as follows:

$$[(C_0/J)I + D_\xi^- \hat{A}^+ + D_\xi^+ \hat{A}^-](J/C_0)[(C_0/J)I + D_\xi^- \hat{B}^+ + D_\xi^+ \hat{B}^-]\Delta Q^p = -(1/J)(C_0 Q^{n+1,p} + C_1 Q^n + C_2 Q^{n-1}) - [D_\xi(\hat{E} - \hat{E}_v) + D_\eta(\hat{F} - \hat{F}_v)] \tag{2}$$

In Eq. (2) the coefficients C_0, C_1, and C_2 are calculated by changing the time-step size at each computing step

$$C_0 = \frac{1 - \sigma}{(1 - \sigma)\Delta t_2 + \Delta t_1}, \qquad C_1 = \frac{\sigma}{(1 - \sigma)\Delta t_2 + \Delta t_1}$$
$$C_2 = \frac{-1}{(1 - \sigma)\Delta t_2 + \Delta t_1} \sigma = \left(1 + \frac{\Delta t_1}{\Delta t_2}\right) \tag{3}$$
$$\Delta t_1 = t^n - t^{n-1}, \qquad \Delta t_2 = t^{n+1} - t^n$$

The inviscid fluxes in RHS are evaluated using a flux difference splitting (FDS) scheme. Third-order spatial accuracy is obtained using the MUSCL approach with a minmod limiter. The turbulence effect is incorporated using the Baldwin–Lomax model with a relaxation length modification and only finding the F_{max} value in a boundary layer in a highly vortical region. Transition is fixed at 0.075 chord from the leading edge according to the experimental data.

Grid Method

For the multizone solver the grid for the spoiler is generated independently and overset onto the main airfoil grid. The cell containing an interpolation point of another grid is found and the contribution of each vertex is calculated based on the bilinear interpolation method. The accuracy of intergrid communication usually depends on the quality of the grid at the interpolation region rather than whether the interpolation is conservative or not.[16] The problems related to the grid deformation are the accurate discovery of a new grid position and grid speed at each time step, and the incorporation of the effect of cell area change. The present dynamic grid method can efficiently find new deformed grid positions and grid speeds analytically without any interpolation or parabolic sheared transformation. If the boundary grid line is determined with a suitable method, internal grid position and velocity can be determined by describing the grid line motion as a sequence of translational, expansional, and rotational motions as illustrated in Fig. 1. Internal grid positions at the new time step are determined as follows:

$$\begin{Bmatrix} x_j \\ y_j \end{Bmatrix} = \begin{Bmatrix} x_b \\ y_b \end{Bmatrix}^{n+1} + \begin{bmatrix} e & 0 \\ 0 & e \end{bmatrix} \begin{bmatrix} \cos\theta & -\sin\theta \\ \sin\theta & \cos\theta \end{bmatrix} \begin{Bmatrix} x_j - x_b \\ y_j - y_b \end{Bmatrix}^n \tag{4}$$

where the expansion ratio e and rotation angle θ are determined from the transformation of the boundary vector of the grid line

$$e = l^{n+1}/l^n, \qquad \cos\theta = \frac{\boldsymbol{l}^n \cdot \boldsymbol{l}^{n+1}}{|\boldsymbol{l}^n||\boldsymbol{l}^{n+1}|} \tag{5}$$

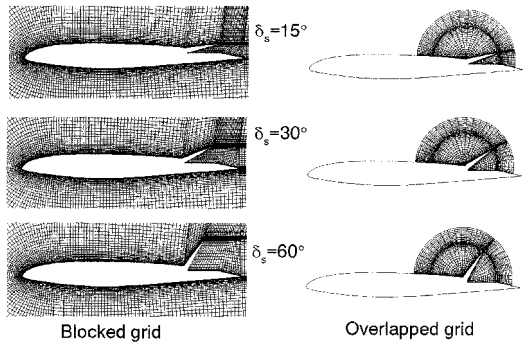

Fig. 2 Comparison of blocked grid system with overlapped grid system around an airfoil with spoiler.

To determine inner grid velocity and grid velocity at boundary b, f is split into each component of motion. If we assign the velocity at b as a translational velocity, relative velocity at f about b is composed of expansion velocity and rotation velocity. Hence, expansion velocity at f is expressed as

$$(\boldsymbol{X}_\tau)_E = \{[(\boldsymbol{X}_\tau)_f - (\boldsymbol{X}_\tau)_b]\cdot\hat{\boldsymbol{u}}_t\}\hat{\boldsymbol{u}}_t \tag{6}$$

rotational velocity at f is

$$(\boldsymbol{X}_\tau)_R = (\boldsymbol{X}_\tau)_f - (\boldsymbol{X}_\tau)_b - (\boldsymbol{X}_\tau)_E \tag{7}$$

angular velocity about b is

$$\boldsymbol{\Omega} = (\hat{\boldsymbol{u}}_t/|\boldsymbol{l}|) \times (\boldsymbol{X}_\tau)_R \tag{8}$$

Finally, inner grid velocity at j is expressed as

$$(\mathbf{X}_\tau)_j = (\boldsymbol{X}_\tau)_b + \boldsymbol{\Omega}\times(\boldsymbol{X}_j - \boldsymbol{X}_b) + \frac{(\boldsymbol{X}_\tau)_E\cdot\hat{\boldsymbol{u}}_t}{|\boldsymbol{l}|}[l_j^t\hat{\boldsymbol{u}}_t + l_j^n(\hat{\boldsymbol{u}}_n)_j] \tag{9}$$

where the expansion velocity at j because of $(\boldsymbol{X}_\tau)_E$ is proportional to the tangential and normal expansion ratio.

The present work has coupled the preceding deformable dynamic grid method with a chimera grid scheme. Hence, the present overlapped flexible dynamic grid method contains the merits of both a chimera and dynamic grid. Figure 2 presents both types of blocked and overset grids around an airfoil with a spoiler. In the present calculations a blocked grid was also used in case of a stationary spoiler. The subgrid around a spoiler moves like an folding–unfolding fan when the spoiler oscillates. This configuration has no constraints on a small spoiler deflection angle. Because the shape of the far boundary is a circle, an analytic dynamic grid description is possible in the far boundary grid. In addition, it can be successfully applied to the two body-connected relative motion problems such as a large displacement motion of the spoiler and a two-body, partly separated problem.

One inevitable problem of a flexible grid method is the exact description of the cell area change effect known as a geometric conservation law (GCL). GCL was originally proposed by Thomas and Lombard[18] and has been modified to a suitable form with Eq. (2) and is described as follows:

$$\frac{\partial}{\partial\tau}\left(\frac{1}{J}\right)^{n+1} = -\left[\frac{\partial}{\partial\xi}\left(\frac{\xi_t}{J}\right) + \frac{\partial}{\partial\eta}\left(\frac{\eta_t}{J}\right)\right]^{n+1} \equiv -RHS_{\mathrm{GCL}}^{n+1}$$
$$\left(\frac{1}{J}\right)^{n+1} = -\frac{C_1}{C_0}\left(\frac{1}{J}\right)^{n} - \frac{C_2}{C_0}\left(\frac{1}{J}\right)^{n-1} - \frac{1}{C_0}RHS_{\mathrm{GCL}}^{n+1} \tag{10}$$

Results and Discussion

NACA 0012 Pitching Motion

To verify time accuracy and an overlapped flexible dynamic grid method, a NACA 0012 airfoil performing pitching oscillation is solved. Rigid grid motion corresponds to the whole grid system move as an equation of motion; whereas in flexible grid motion far boundary is fixed and the inner cell is deformed as the body moves. Figure 3 compares the variation of unsteady aerodynamic coefficients. The results of the present overlapped dynamic grid method agree well with experimental data, exact (rigid) single-grid motion, and chimera grid with exact grid motion. Also shown in Fig. 3 is the effect of GCL. When GCL is applied the result is almost identical to that of rigid grid solution. Hence, this flexible dynamic grid method is accurate and efficient in a single grid as well as a Chimera grid.

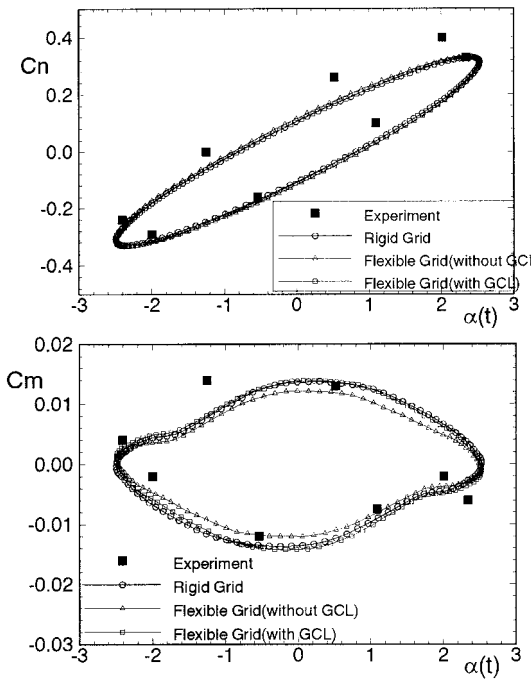

Fig. 3 Comparison of unsteady aerodynamic loads of pitching NACA 0012 airfoil [$\alpha = \alpha_0 + \alpha_m \sin(2M_\infty K\tau)$, $M_\infty = 0.755$, $\alpha_0 = 0.016$ deg, $\alpha_m = 2.5$ deg, and $K = 0.0814$].

Stationary Spoiler

The basic calculation model is based on a BATR airfoil. A spoiler of 0.1554 chord length is hinged 0.733 chord from the leading edge. This configuration has been studied experimentally by many researchers. Computations were carried out at $M_\infty = 0.13$ and $Re = 2.8 \times 10^5$. The spoiler deflection angle is 15, 30, and 60 deg, and the airfoil of attack is 0 deg. The calculation was initiated with freestream conditions and continued until periodic vortex shedding was reached. The nondimensional time step was chosen as 0.02, and the second-order time accuracy was preserved with 2-N subiterations.

Mean pressure distributions are shown in Fig. 4. The typical pressure distribution of an airfoil with a deflected spoiler is the suction on the upper surface upstream of the spoiler, and the pressure on the lower surface decreases as δ_s increases but the constant suction downstream of the spoiler (base pressure) increases with δ_s. However, the gain in the base pressure region is less than the loss of the suction upstream of the spoiler on the upper surface; therefore, total lift decreases with δ_s. Figure 4 represents this phenomena well and favorable agreement is achieved with the experimental data of Lee and Bodapati.[7] Some discrepancy on the upper surface near the trailing edge can be attributed to the slight difference in geometry with experimental data and the limitation of an algebraic turbulence model in spite of modifications in the highly vortical region as suggested by Degani.[21] Caution should be taken when the comparison is made because these experimental data were not corrected wind-tunnel blockage effects. The time-averaged lift and drag characteristics are shown in Fig. 5. The

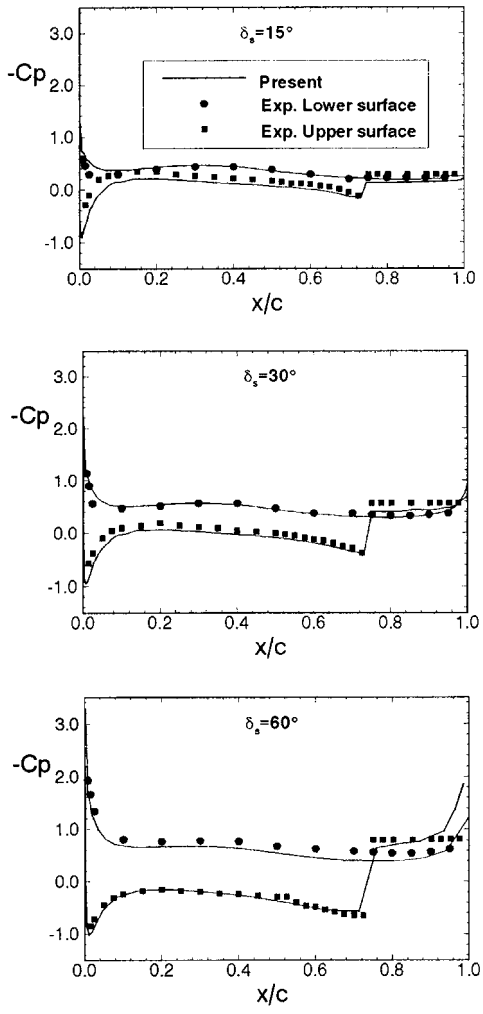

Fig. 4 Comparison of the time-averaged pressure coefficients vs spoiler deflection angle (M_∞ = 0.13, Re = 2.8 × 10^5, and α = 0 deg).

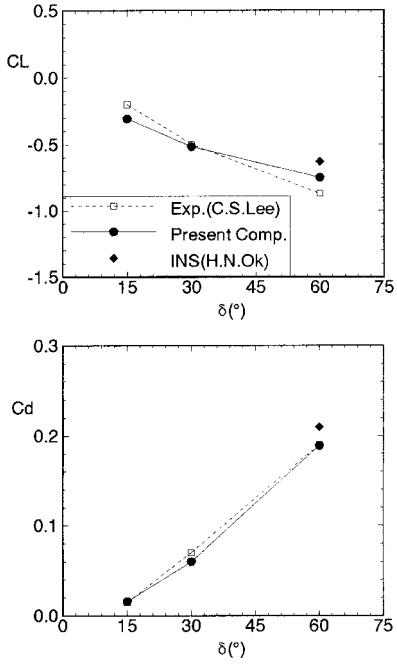

Fig. 5 Comparison of the time-averaged lift and drag coefficients vs spoiler deflection angle (M_∞ = 0.13, Re = 2.8 × 10^5, and α = 0 deg).

lift decreases and the drag increases with increasing spoiler deflection. This is in good agreement with experimental data except for small-deflection angles. Vortex shedding and pressure oscillation on the surface are the characteristic features of an airfoil with a deflected spoiler. The character of vortex shedding is disclosed in Fig. 6 and the shedding frequency is determined from the Fourier transform of time history data to the frequency domain. It is evident that the shedding frequency decreases and that the fluctuation level increases with increasing spoiler deflection angle. This is consistent with the results of the general bluff body in that the vortex shedding frequency is inversely proportional to the width of the wake of the body. Also, of note is that at a higher spoiler deflection the band of peak amplitude of the surface pressure is narrow, and with decreasing spoiler deflection the band widens. This character was also observed in the experiment by McLachlan et al.[6] With regard to the appropriate characteristic length of the Strouhal number, it was proposed that the spoiler projection height above the airfoil trailing edge is more appropriate than the airfoil chord length.[3,6] This definition is similar to Griffin and Hall's[19] universal wake Strouhal number. Figure 7 confirms their statements and shows good agreement with the present computations.

The vortex shedding induces a fluctuating pressure field over the surface of the airfoil and Fig. 8 illustrates the chordwise distribution of peak values of a pressure spectra. All peak values correspond to the vortex shedding frequency of aerodynamic coefficient spectra. This also confirms the validity of the estimation of the shedding frequency from the lift history or

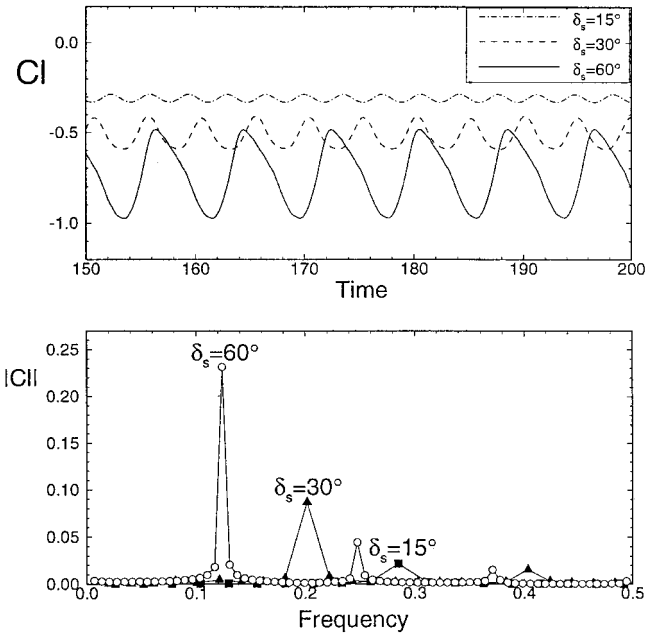

Fig. 6 Time history and frequency spectra of aerodynamic coefficients (M_∞ = 0.13, Re = 2.8 × 10^5, and α = 0 deg).

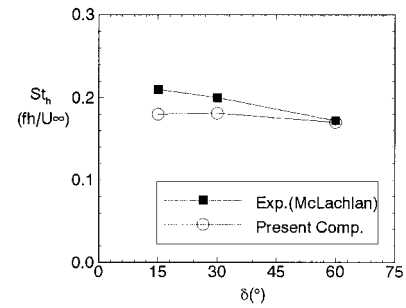

Fig. 7 Comparison of Strouhal number vs spoiler deflection angle (M_∞ = 0.13, Re = 2.8 × 10^5, and α = 0 deg).

one point wake velocity measurement in the experiment. The fluctuating pressure of the upper surface has local maximum in an airfoil's leading edge and increases steadily upstream of the spoiler. This is followed by an abrupt increase in the spoiler trailing edge and constant near-base region. Near the airfoil's trailing edge this fluctuation increases sharply as one order of magnitude larger than that of the leading-edge region. In the lower surface the level of the fluctuation increases steadily from the leading edge to the trailing edge. In Fig. 9 one period of vortex shedding at a spoiler deflection angle of 60 deg is simulated. Of note is that the period of lift oscillation is the same as that of the visualized streamline plot. At the instant of maximum lift, spoiler-tip vortex is dominant on the base region. This vortex causes the lower pressure on the base region, where maximum lift occurred. This counterclockwise vortex also induces secondary vortex in the corner region. It is also shown that a mild hinge bubble is formed upstream of the spoiler. The suction on the base region causes the development of the trailing-edge vortex. Pressure increases on the base region as the trailing vortex develops, thus lift decreases gradually. At the minimum lift point, a pair of vortex exists that originated from the spoiler tip and the airfoil's trailing edge. The growing of the trailing-edge vortex is restricted by the spoiler-tip vortex, and so the trailing-edge vortex is shed and dissipated to a weak vortex. As a result, the lift increases again. This vortex shedding mechanism is repeated periodically. Although not shown here, at a small deflection angle the merging of the corner vortex and the two vortices (spoiler-tip vortex and trailing-edge vortex) was observed. The decreased regularity of vortex shedding at a small deflection angle observed in the experiment may be a result of this vortex shape. However, numerical results showed no intermittency.

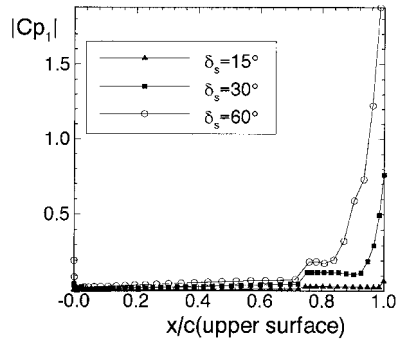

Fig. 8 Distribution of surface pressure fluctuation peak at shedding frequency (M_∞ = 0.13, Re = 2.8 × 10^5, and α = 0 deg).

Oscillating Spoiler

As stated earlier, the flow around an airfoil with a stationary spoiler oscillates because of the periodic vortex shedding in the wake region. The frequencies of flow variables are the same with the vortex shedding frequency and these frequencies are uniform over near flowfield. However, when the spoiler oscillates the flow has two time scales; that is, the time scales of vortex dynamics and of motion. The features of this type of flow are governed by the relative size of two time scales. If the time scales of the motion is long compared to the vortex dynamics, then it is possible to assume the flowfield as quasisteady state. On the other hand, when the time scale of motion is comparable to that of vorticity, the situation is entirely different from the quasisteady case. The dynamic stall vortex generated on the rapidly pitching or ramp motion of an airfoil is of the latter time scale. Some experimental studies concerning oscillating spoilers were performed at the relatively low reduced frequency. However, the frequency can barely change the intrinsic vortex shedding frequency of the stationary spoiler. An experiment in high frequency is difficult and expensive because of the technology required to control the unsteady flow. Hence, in the present work the computational investigations are conducted to enhance the understanding of physics of unsteady flow induced by the oscillating spoiler. The chosen frequency ranges are near that of the vortex shed-

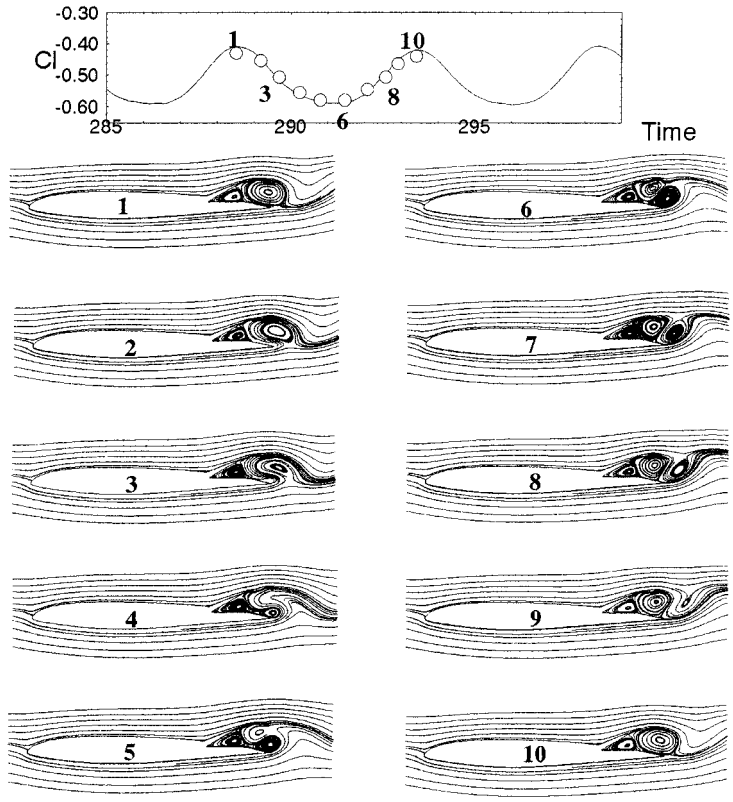

Fig. 9 Streamline patterns during a vortex shedding cycle for δ_s = 60 deg (M_∞ = 0.13, Re = 2.8 × 10^5, α = 0 deg, and an airfoil with a stationary spoiler).

ding frequency of the stationary spoiler. Calculations were carried out on the same flow conditions and geometry with the previous case of the stationary spoiler. The motion of the spoiler is assumed to perform small-amplitude harmonic oscillation, described as

$$\delta(t) = \delta_m + \delta_i \sin(M_\infty KtC/C_s) \tag{11}$$

where the reduced frequency K is based on the spoiler chord length ($K = 2\pi f C_s/U_\infty$) and corresponds to the 0.5, 1, and 2 times the flow frequency generated by the stationary spoiler; that is K is 0.47, 0.94, and 1.98. The mean deflection angle is 60 deg and the amplitudes of oscillation varies as 2, 5, and 10 deg. Figure 10 represents the mean aerodynamic coefficients variation caused by the spoiler's oscillation. When the reduced frequency of the spoiler is less than the convection frequency (the Strouhal frequency of the stationary spoiler), the mean lift and drag decreases. However, when the forced frequency is equal to the convection frequency there is a sudden increase in aerodynamic force, and the tendency is more severe as the amplitude of oscillation increases. This corresponds to the vortex lock-on resonance that occurs when the vortex and vibra-

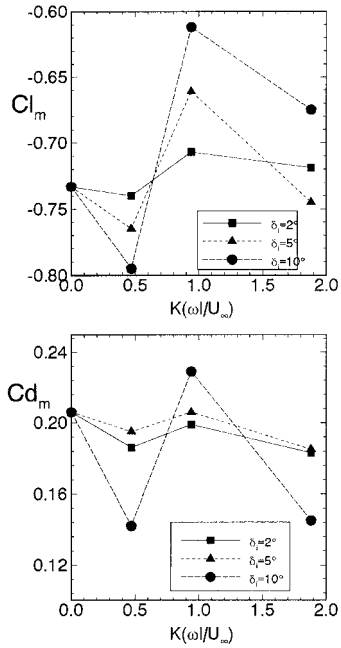

Fig. 10 Variation of mean aerodynamic coefficients with reduced frequency and oscillation amplitude ($M_\infty = 0.13$, $Re = 2.8 \times 10^5$, and $\alpha = 0$ deg).

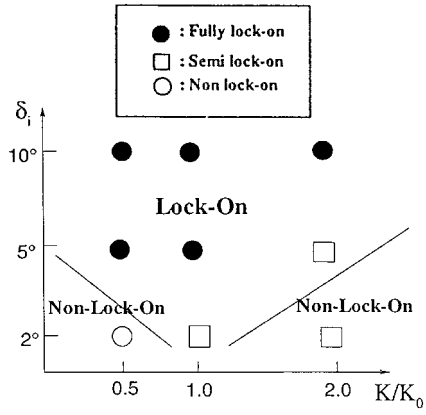

Fig. 11 Limits of lock-on regime as a function of amplitude and frequency for spoiler harmonic oscillation [$\delta(t) = \delta_m + \delta_i \sin(M_\infty K\tau C/C_s)$, $M_\infty = 0.13$, $Re = 2.8 \times 10^5$, and $\alpha = 0$ deg].

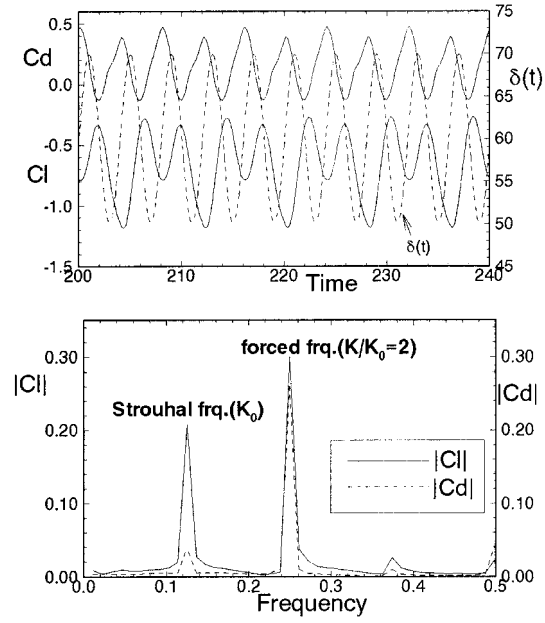

Fig. 12 Time history and frequency spectra of lift and drag in an oscillating spoiler ($K/K_0 = 2.0$, and $\delta_i = 10$ deg).

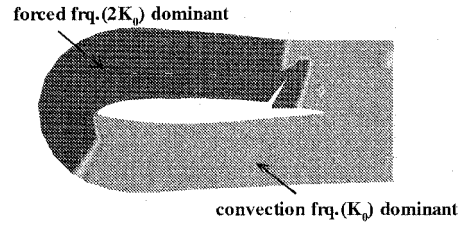

Fig. 13 Dominant frequency distribution around an airfoil with an oscillating spoiler [$M_\infty = 0.13$, $Re = 2.8 \times 10^5$, $\alpha = 0$ deg, $\delta(t) = \delta_m + \delta_i \sin(M_\infty K\tau C/C_s)$, $\delta_i = 10$ deg, and $K/K_0 = 2$].

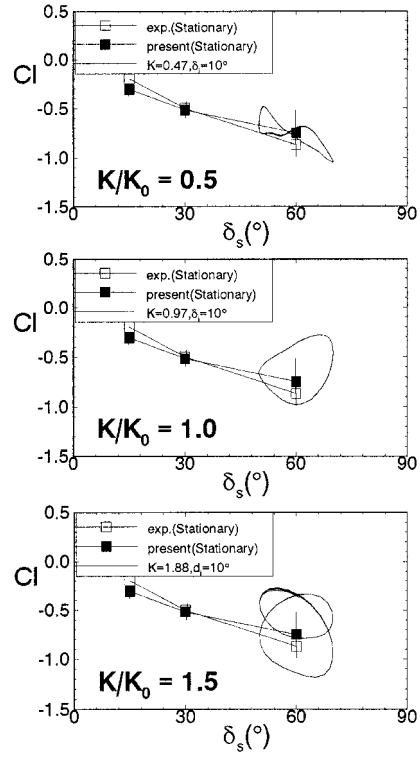

Fig. 14 Phase plot of lift with reduced frequency variation at $\delta_i = 10$ deg.

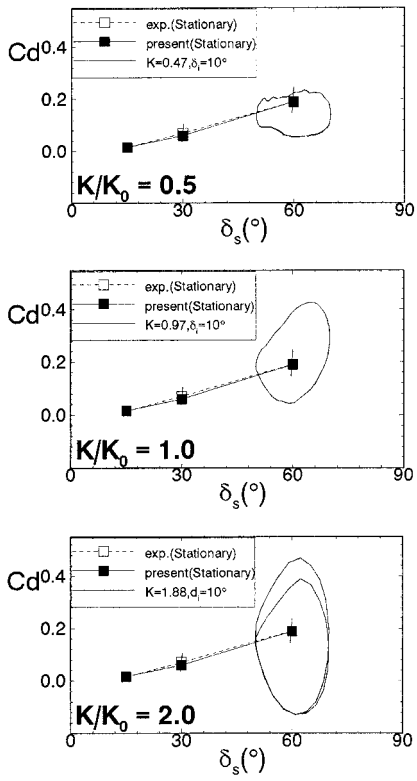

Fig. 15 Phase plot of drag with reduced frequency variation at δ_i = 10 deg.

tion frequency are coincident.[19] If a bluff body is flexible and lightly damped, then the resonant oscillations can be excited by the incident flow. As a consequence of this flow-induced resonance the body and wake oscillations attain the same frequency, which is near one of the characteristic frequencies of the structures.[19] Conversely, the lock-on resonance is also induced when a rigid body is forced to oscillate over the appropriate range of imposed frequencies and amplitudes. In many cases the lock-on frequency is near Strouhal frequency and the present computations captured this phenomenon. Figure 11 represents limits of the lock-on regime as functions of amplitude and frequency for spoiler harmonic oscillation. The lock-on state is determined from the existence of the limit cycle of lift curve on deflection angle variation. Typical V-shaped lock-on regime can be seen as general bluff-body oscillation and this regime increases as amplitude increases. As stated earlier, if the forced frequency is different from the convection frequency, the flow has two time scales. The dominance depends on the level of the forced oscillation. The time history of lift in Fig. 12 represents such two time scales. If the time signal is Fourier transformed two dominant frequencies are clearly seen. The amplitude at each frequency varies with level of the oscillation and the dominant frequency is not uniform over the flowfield. Figure 13 represents dominant frequency distribution. As the oscillation amplitude increases, the portion of flowfield in which the forced oscillation is dominant enlarges. A distinctive feature to note is that upstream of the spoiler the upper surface is influenced more by the oscillation of the spoiler but the influence is not so significant in the wake region. The small-scale vortex that retains the forced frequency is recovered to a large-scale vortex of convection frequency,

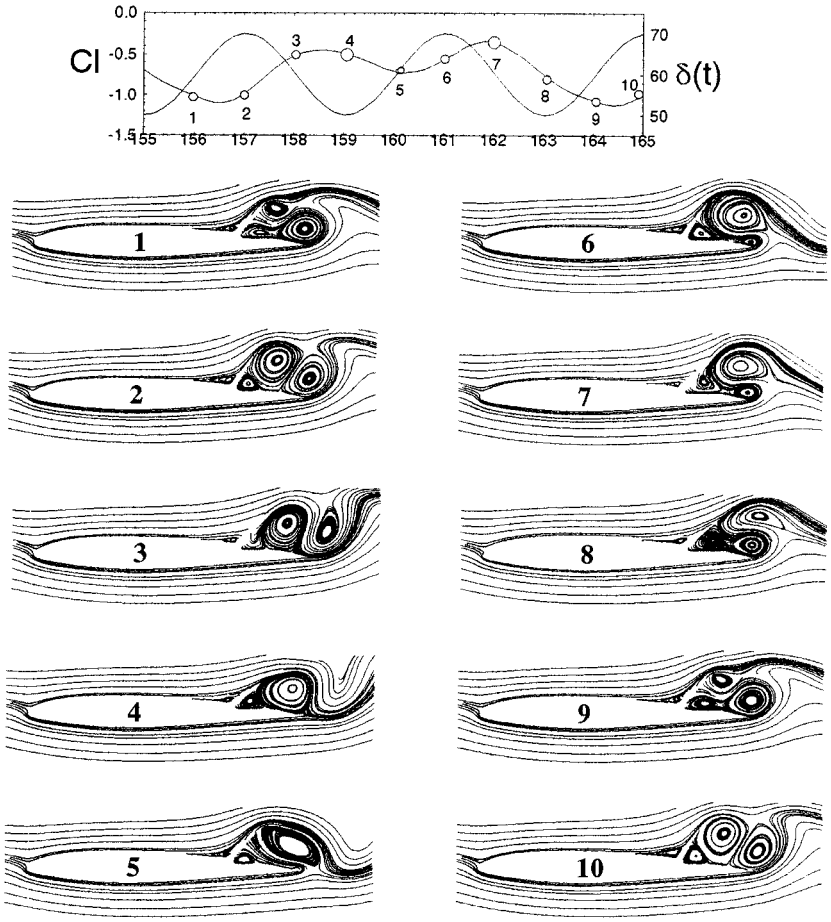

Fig. 16 Streamline patterns around an airfoil with an oscillating spoiler [$\delta(t) = \delta_m + \delta_i \sin(M_\infty K\tau C/C_s)$, δ_i = 10 deg, and K/K_0 = 2.0].

and this recovered convection frequency is almost identical to the Strouhal frequency of a stationary spoiler. Figure 14 shows the phase-plane plot of lift for each reduced frequency. The lift response shows a hysteresis effect similar to the effect obtained on an oscillating airfoil with an angle of attack. Figure 14 shows that the level of lift fluctuation also increases as the reduced frequency increases, and that is considerably different from the corresponding stationary value. Note that when the forced frequency is the same as the convective frequency, the hysteresis loops show a single curve. In other cases, the hysteresis loop shows what is essentially a second harmonic lift variation that results from the two dominant frequencies. The corresponding unsteady drag plot is shown in Fig. 15. As the reduced frequency increases, the fluctuating drag also increases. In case the frequency ratio is equal, the mean drag is above the corresponding stationary value. At the highest reduced frequency of this study, an unexpected phenomena was observed in which oscillation produced the negative drag, i.e., thrust. This phenomenon was found to be a result of a large suction on the rear surface of the spoiler when the spoiler moves up. This phenomenon is known as the *Katzmayr effect* occurring in an airfoil moving through a sinusoidal upwash field or a plunging airfoil.[20]

The vortex shedding behind an oscillating spoiler is represented in Fig. 16. A salient feature of an oscillating spoiler vortex is that oscillation caused a stronger spoiler tip vortex than a stationary spoiler did. The development of a trailing-edge vortex is temporally delayed by the motion of the spoiler. When spoiler moves up, indicated as 6 and 7 in Fig. 16, strong suction on the rear surface of the spoiler appears. This suction delays the shedding of the spoiler-tip vortex and the development of the trailing-edge vortex. Therefore, the lift history has local minimum at state 5. This visualization of vortex shedding suggests that the upwind motion of the spoiler affects the temporal increase in lift. Moreover, this temporal increase in lift is accompanied by the temporal negative drag, that is, thrust as shown in Fig. 15. If more rapid and larger amplitudes of the spoiler motion is given, the strong vortex will be generated on the rear surface of the spoiler. This dynamic vortex may cause a more severe lift increase than that shown in Fig. 16. This also indicates that the oscillating spoiler has potential capabilities for the application of ACT. On the contrary a downward motion of the spoiler enhanced the development of the trailing-edge vortex, thus lift decreased rapidly. If a different type of motion, that is, one of the periodic sawtooth, pitch-and-hold or higher harmonic oscillations is applied, this undesirable effect could be removed.

Concluding Remarks

Time-accurate solutions of the Navier–Stokes equations on the flowfield around an airfoil with a stationary or oscillating spoiler have been obtained using the FDS scheme, the ADI scheme with Newton subiteration, and an overlapped dynamic grid method. The unsteady flow around a stationary spoiler with various deflection angles has been computed and it showed good agreement with existing experimental data. The overlapped dynamic grid method has been well applied to the oscillatory spoiler problem and the method permits the analysis of the relative grid motion, particularly the motion between two contacted bodies with large grid deformations. The unsteady flow around an oscillating spoiler depends on the frequency ratio between oscillation and Strouhal frequencies and the length scale ratio between the amplitude of oscillation and the vortex length scale. Low-frequency oscillation can reduce a fluctuating load, and so it contributes to the suppression of structural vibration. Whereas high-frequency oscillation induces dynamic stall vortex, this large unsteady aerodynamic load can be used for the application of ACT.

The present computation will contribute to the better understanding of the vortical flow phenomena around an airfoil with a spoiler and the improvement of the methodology in analyzing the unsteady flow induced by the relative motion between two contacted bodies.

Acknowledgment

This work was supported, in part, by the Ministry of Science and Technology in Korea.

References

[1]Cole, S. R., "Aeroelastic Effects of Spoiler Surfaces on a Low Aspect Ratio Rectangular Wing," *Journal of Aircraft*, Vol. 29, No. 5, 1992, pp. 768–773.

[2]Wentz, W. H., Ostowari, C., and Seetharam, H. C., "Effects of Design Variables on Spoiler Control Effectiveness, Hinge Moments and Wake Turbulence," AIAA Paper 81-0072, Jan. 1981.

[3]Bodapati, S., Mack, M. D., and Karamcheti, K., "Basic Studies of the Flow Fields of Airfoil-Flap-Spoiler Systems," AIAA Paper 82-0173, Jan. 1982.

[4]Ayoub, A., Bodapati, S., Karamcheti, K., and Seetharam, H. C., "Unsteady Flow Patterns Associated with Spoiler Control Devices," AIAA Paper 82-0127, Jan. 1982.

[5]McLachlan, B. G., Karamcheti, K., and van Leynseels, F., "Experimental Study of the Flowfield of an Airfoil with Deflected Spoiler," AIAA Paper 82-0126, Jan. 1982.

[6]McLachlan, B. G., Karamcheti, K., Ayoub, A., and Hadjidakis, G., "A Study of the Unsteady Flowfield of an Airfoil with Deflected Spoiler," AIAA Paper 83-2131, Aug. 1982.

[7]Lee, C. S., and Bodapati, S., "Experimental Investigations of the Flowfield of an Airfoil with Spoiler," *AIAA Journal*, Vol. 25, No. 11, 1987, pp. 1411–1416.

[8]Ok, H. N., and Eberhardt, D. S., "Calculation of the Flowfield Around an Airfoil with Spoiler," AIAA Paper 93-0527, 1993.

[9]Costes, M., Gravelle, A., and Philippe, J. J., "Investigation of Unsteady Subsonic Spoiler and Flap Aerodynamics," *Journal of Aircraft*, Vol. 24, No. 9, 1987, pp. 629–637.

[10]Consigny, H., Gravelle, A., and Molinaro, R., "Aerodynamic Characteristics of a Two Dimensional Moving Spoiler in Subsonic and Transonic Flow," *Journal of Aircraft*, Vol. 21, No. 9, 1984, pp. 687–693.

[11]Nelson, C. F., Koga, D. J., and Eaton, J. K., "Unsteady Separated Flow Behind an Oscillating Two-Dimensional Flap," AIAA Paper 89-0288, Jan. 1989.

[12]Jordan, F. L., Jr., Gato, W., Masiello, M. F., O'Rourke, M., and White, E. R., "Experimental Investigation of Unsteady Aerodynamics on a Flap Element Induced by Rapid Spoiler Deflection," AIAA Paper 94-1886, June 1994.

[13]Mabey, D. G., "Review of Some Recent Research on Time-Dependent Aerodynamics," *Aeronautical Journal*, Vol. 88, Feb. 1984, pp. 23–37.

[14]Mabey, D. G., "On the Prospects for Increasing Dynamic Lift," *Aeronautical Journal*, Vol. 92, March 1988, pp. 95–106.

[15]Weeratunga, S. K., Barszcz, E., and Chawla, K., "Moving Body Overset Grid Applications on Distributed Memory MIMD Computers," AIAA Paper 95-1751, June 1995.

[16]Meakin, R. L., "On the Spatial and Temporal Accuracy of Overset Grid Methods for Moving Body Problems," AIAA Paper 94-1925, June 1994, pp. 858–871.

[17]Kim, C. J., and Lee, D. H., "Time Accurate Computation of Unsteady Transonic Flows Around an Airfoil with Oscillating Flap on Dynamic Grid," AIAA Paper 92-2733, June 1992.

[18]Thomas, P. D., and Lombard, C. K., "Geometric Conservation Law and Its Application to Flow Computations on Moving Grid," *AIAA Journal*, Vol. 17, No. 10, 1979, pp. 1030–1037.

[19]Griffin, O. M., and Hall, M. S., "Review-Vortex Shedding Lock-on and Flow Control in Bluff Body Wakes," *Journal of Fluids Engineering*, Vol. 113, Dec. 1991, pp. 526–537.

[20]Ribner, H. S., "Thrust Imparted to an Airfoil by Passage Through a Sinusoidal Upwash Field," *AIAA Journal*, Vol. 31, No. 10, 1993, pp. 1863–1868.

[21]Degani, D., Schiff, L. B. and Levy, Y., "Numerical Prediction of Subsonic Turbulent Flows over Slender Bodies at High Incidence," *AIAA Journal*, Vol. 29, No. 12, 1991, pp. 2054–2061.